

BUCKLING OF AXIALLY LOADED, LONG RECTANGULAR PAPERBOARD PLATES

*Millard W. Johnson, Jr.*¹

University of Wisconsin, Madison, WI 53706

and

Thomas J. Urbanik

Research General Engineer

Forest Products Laboratory,² Forest Service

U.S. Department of Agriculture, Madison, WI 53705-2398

(Received March 1986)

ABSTRACT

This study examines the elastic buckling of long rectangular plates made of paper and subjected to compressive axial loading. The model is appropriate for the facing and flute components of corrugated fiberboard. A dimensionless stiffness, S , and mean Poisson's ratio, ν , characterize the dimensions of the plate and the nonlinear orthotropic stress-strain relation of paper. The dimensionless buckling stress $\hat{\sigma}$ depends on S , ν , and the plate edge condition, which can be fixed or simply supported. An examination of $\hat{\sigma}$ versus S predicts the stiffness needed to prevent elastic buckling and shows how the significance of edge restraint and material nonlinearity vary with S . An iterative solution is given for doing the analysis. Comparing the results obtained assuming fixed edges to those obtained assuming simply supported edges explains how fiberboard strength may vary due to component variations. Comparing the results obtained for nonlinear materials to those obtained for linear materials explains why fiberboard edgewise compressive strength cannot be accurately predicted from only the components' strengths.

Keywords: Plates, elastic stability, buckling, corrugated fiberboard, paper, material failure, edgewise compression.

INTRODUCTION

In this study we consider theoretically the elastic buckling of long rectangular paperboard plates under compressive loading in the longitudinal, y -direction. Shear, lateral, i.e., x -direction, or other loads such as bending and twisting are not considered. Two conditions of rotational edge restraint are considered: Longitudinal edges either both simply supported or both fixed, and both edges restrained from lateral movement. The solution is based on equations, derived by Johnson and Urbanik (1984), for the nonlinear deformation of plates of paper material. Their theory incorporates the nonlinear orthotropic material behavior of paper. Aside from our consideration of paper, the results of this study by themselves contribute to the literature of plate theory.

A paperboard section of corrugated board having edges coinciding with the

¹ Supported by National Science Foundation under Grant No. MEA-8120393 (Clifford J. Astill, Program Director).

² The Laboratory is maintained in cooperation with the University of Wisconsin. This article was written and prepared by U.S. Government employees on official time, and it is therefore in the public domain (i.e., it cannot be copyrighted).

gluelines can be considered as a long thin plate if the effects of curvature induced by the corrugating operation are small and can therefore be neglected. The edge condition is considered elastic, i.e., intermediate between fixed and simple support, due to the mutual restraint between facings and flutes. Hence, in these fiberboard structures the failure stresses due to elastic instability would be bounded by the results from our analysis.

Paperboard plates are considered under longitudinal loading when the fiberboard is compressed parallel to the flutes. The longitudinal loading condition considered here is typically in the paper's cross direction (CD), but the parameters of this theoretical analysis can be switched to investigate machine-direction (MD) loading.

This study was motivated by our earlier work (Johnson et al. 1979) in which we showed how to calculate the edgewise compressive strength of single-wall fiberboard. Simplifying assumptions in that work limited its scope to isotropic paperboard components in the flutes and both facings. The results were a method for optimally matching components based on the stress-strain relations and predicted failure modes. Lightweight paper combinations were found to trigger local instability while heavyweight paper combinations resulted in compression being the failure mechanism. The optimal design with minimum fiber weight was when both facings and flutes simultaneously initiated structural collapse, be it by local instability or by compression.

The implications for more efficient and effective fiber utilization prompted a more accurate thin-plate theory (Johnson and Urbanik 1984) encompassing nonlinear and orthotropic paper behavior. The expression proposed in Johnson and Urbanik (1984) for the edgewise compression of paper in the cross direction is

$$\sigma(\epsilon) = c_1 \tanh(c_2 \epsilon / c_1) \quad (0.1)$$

where σ is the stress, ϵ is the strain, and c_1 and c_2 are material constants. Equation (0.1) is written for the cross direction of the paper so that constants c_1 and c_2 are appropriate to that direction. The same form of relation with different material constants holds for uniaxial compression in any direction. Using Eq. (0.1), the theory given in Johnson and Urbanik (1984) yields an expression for the strain energy on which a general biaxial theory is based.

As specifications for corrugated fiberboard change from material to performance criteria, the ability of paperboard to remain elastically stable under edgewise loading warrants increased attention. Manufacturers need to alter paper-weight combinations to optimally match strength and cost considerations. Advanced concepts in papermaking, and additives designed to resist moisture or other environmental detriments, have led to lighter-weight paperboards that perform as well as the heavier-weight paperboards they replaced. Consumers, motivated by economic benefits, increasingly supplement the fiberboard burst specification with their own specification based on edgewise compressive strength. The results of this analysis complement our earlier work (Johnson et al. 1979) and expand the knowledge on how to consider paper as an element in a sandwich structure.

BASIC EQUATIONS

We use the equation of equilibrium written in the form of Eq. (2.37) of Johnson and Urbanik (1984) for no surface load, $q = 0$.

$$\begin{aligned} \frac{\partial^2 M_{11}}{\partial x^2} + 2 \frac{\partial^2 M_{12}}{\partial x \partial y} + \frac{\partial^2 M_{22}}{\partial y^2} + \frac{\partial}{\partial x} \left(N_{11} \frac{\partial W}{\partial x} + N_{12} \frac{\partial W}{\partial y} \right) \\ + \frac{\partial}{\partial y} \left(N_{22} \frac{\partial W}{\partial y} + N_{21} \frac{\partial W}{\partial x} \right) = 0 \end{aligned} \quad (1.1)$$

Here, x and y are material Cartesian coordinates, N_{ij} force resultants, M_{ij} moment resultants, and W the transverse displacement component. The moment curvature relations are given by Eq. (2.34) of Johnson and Urbanik (1984).

$$\left. \begin{aligned} M_{11} &= -\frac{1}{12} h^3 \left[H_{11} \frac{\partial^2 W}{\partial x^2} + H_{12} \frac{\partial^2 W}{\partial y^2} + H_{13} \frac{\partial^2 W}{\partial x \partial y} \right] \\ M_{22} &= -\frac{1}{12} h^3 \left[H_{12} \frac{\partial^2 W}{\partial x^2} + H_{22} \frac{\partial^2 W}{\partial y^2} + H_{23} \frac{\partial^2 W}{\partial x \partial y} \right] \\ M_{12} &= -\frac{1}{24} h^3 \left[H_{13} \frac{\partial^2 W}{\partial x^2} + H_{23} \frac{\partial^2 W}{\partial y^2} + H_{33} \frac{\partial^2 W}{\partial x \partial y} \right] \end{aligned} \right\} \quad (1.2)$$

where H_{ij} are the bending stiffness moduli, which are functions of the middle surface strains, and h is the plate thickness.

For compression in the y -direction of the plate, the bending stiffness moduli are given by Eq. (4.9) of Johnson and Urbanik (1984).

$$\left. \begin{aligned} H_{11} &= \frac{c_1 \nu_1 / \nu_2}{1 - \nu_1 \nu_2} \frac{\tanh(c_2 \epsilon / c_1)}{\epsilon} \\ H_{22} &= \frac{c_2}{\cosh^2(c_2 \epsilon / c_1)} + \frac{\nu_1 \nu_2 c_1}{1 - \nu_1 \nu_2} \frac{\tanh(c_2 \epsilon / c_1)}{\epsilon} \\ H_{12} &= \frac{c_1 \nu_1}{1 - \nu_1 \nu_2} \frac{\tanh(c_2 \epsilon / c_1)}{\epsilon} \\ H_{33} &= c H_{12} \\ H_{13} &= H_{23} = 0 \end{aligned} \right\} \quad (1.3)$$

where constant c , which is related to an approximate shear modulus, is given by Eqs. (3.3) and (4.2) of Johnson and Urbanik (1984) as

$$c = \frac{2(1 - \sqrt{\nu_1 \nu_2})}{\sqrt{\nu_1 \nu_2}} \quad (1.4)$$

where ν_1 is Poisson's ratio associated with x -direction compression and ν_2 with y -direction compression.

PLATE BUCKLING

The prebuckled plate is in uniform axial compression under the load conditions

$$\begin{aligned} N_{22} &= -N_0 = -hc_1 \tanh(c_2 \epsilon / c_1) \\ N_{11} &= N_{12} = 0 \end{aligned} \quad (2.1)$$

The middle surface strain field is homogeneous so the H_{ij} are independent of x and y . With $H_{13} = H_{23} = 0$ from Eq. (1.3), we substitute expressions (1.2) into (1.1) to obtain the equation for the buckling perturbation W .

$$H_{11} \frac{\partial^4 W}{\partial x^4} + H_{22} \frac{\partial^4 W}{\partial y^4} + (2H_{12} + H_{33}) \frac{\partial^4 W}{\partial x^2 \partial y^2} + \frac{12}{h^3} N_0 \frac{\partial^2 W}{\partial y^2} = 0 \quad (2.2)$$

We consider solutions of Eq. (2.2) of the form

$$W = A_0 e^{i\lambda y + \alpha x} \quad (2.3)$$

Substituting Eq. (2.3) into (2.2) leads to a fourth degree equation for $\alpha(\lambda)$. The four roots are $\alpha, -\alpha, i\beta, -i\beta$ where

$$\alpha = \left\{ \frac{(2H_{12} + H_{33})\lambda^2 + \left[(2H_{12} + H_{33})^2 \lambda^4 - 4H_{11} \left(\lambda^4 H_{22} - \frac{12}{h^3} N_0 \lambda^2 \right) \right]^{1/2}}{2H_{11}} \right\}^{1/2} \quad (2.4)$$

$$\beta = \left\{ \frac{-(2H_{12} + H_{33})\lambda^2 + \left[(2H_{12} + H_{33})^2 \lambda^4 - 4H_{11} \left(\lambda^4 H_{22} - \frac{12}{h^3} N_0 \lambda^2 \right) \right]^{1/2}}{2H_{11}} \right\}^{1/2} \quad (2.5)$$

Instead of Eq. (2.4) we shall use

$$\alpha^2 - \beta^2 = \frac{(2H_{12} + H_{33})\lambda^2}{H_{11}} \quad (2.6)$$

Superposing solutions of the form (2.3) one obtains solutions, even in x , of the form

$$W = [a_1 \cosh \alpha x + a_2 \cos \beta x] e^{i\lambda y} \quad (2.7)$$

and solutions, odd in x , of the form

$$W = [a_3 \sinh \alpha x + a_4 \sin \beta x] e^{i\lambda y}$$

We use the even solutions since they lead to lower buckling loads than the odd solutions.

If α and β are substituted from Eqs. (2.5) and (2.6) into (2.7), and boundary conditions on edges $x = \pm b$ applied, we obtain a transcendental characteristic equation for the buckling strain as a function of the wave number λ . The critical buckling strain for a long plate is obtained by minimizing the buckling strain with respect to λ . Remember, the assumption made here is that the critical buckling modes are of form (2.7). There could be other buckling modes that lead to lower buckling strains, but they have not yet been investigated.

We next want to write Eqs. (2.5) and (2.6) in dimensionless form. Eqs. (1.3) and (1.4) give

$$\left. \begin{aligned} \frac{2H_{12} + H_{33}}{H_{11}} &= \nu_2(2 + c) = 2\sqrt{\nu_2/\nu_1} \\ \frac{H_{22}}{H_{11}} &= \nu_2^2 + \frac{\nu_2}{\nu_1}(1 - \nu^2) \frac{2c_2\epsilon/c_1}{\sinh(2c_2\epsilon/c_1)} \\ \frac{N_0}{hH_{11}} &= \frac{\nu_2}{\nu_1}(1 - \nu^2)\epsilon \end{aligned} \right\} \quad (2.8)$$

where ν is the geometric mean Poisson's ratio,

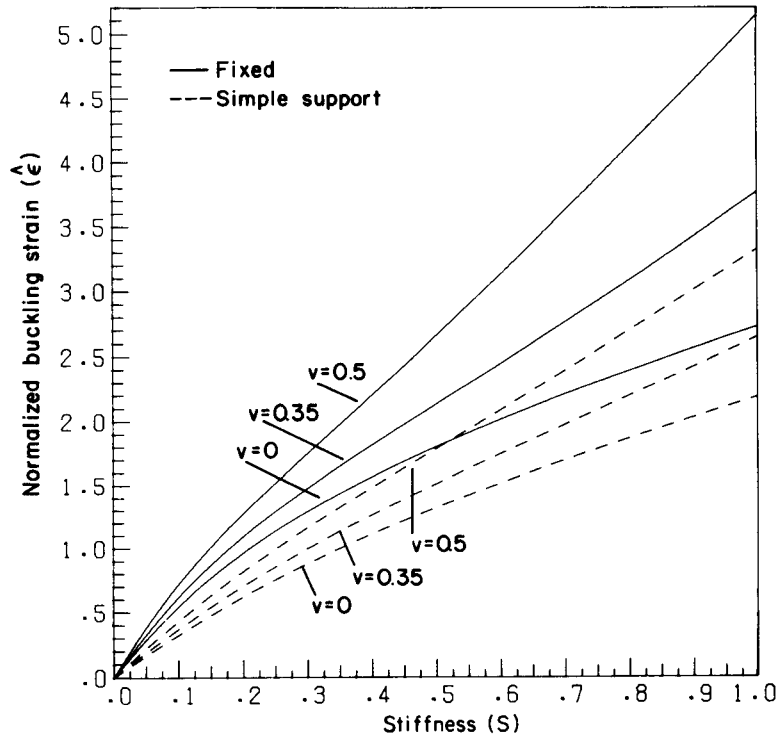


FIG. 1. Plots of $\hat{\epsilon}$ as a function of S for three mean Poisson's ratios and two edge-support conditions. (ML85 5254)

$$\nu = \sqrt{\nu_1 \nu_2} \quad (2.9)$$

Introduce the dimensionless variables:

$$\left. \begin{aligned} \hat{\alpha} &= b\alpha, & \hat{\beta} &= b\beta, & \hat{\epsilon} &= c_2 \epsilon / c_1 \\ \chi &= b\lambda(\nu_2/\nu_1)^{1/4} \\ S &= (c_2/c_1)(h/2b)^2(\nu_1/\nu_2)^{1/2} \end{aligned} \right\} \quad (2.10)$$

Here, χ is a dimensionless wave number and S a dimensionless stiffness coefficient. Substituting expressions (2.8) and dimensionless variables (2.10) into Eqs. (2.5) and (2.6) gives

$$\hat{\beta} = \chi \left\{ -1 + \sqrt{1 - \nu^2} \left[f(\hat{\epsilon}) + \frac{3\hat{\epsilon}}{\chi^2 S} \right]^{1/2} \right\} \quad (2.11)$$

$$\hat{\alpha} = (\hat{\beta}^2 + 2\chi^2)^{1/2} \quad (2.12)$$

where

$$f(\hat{\epsilon}) = 1 - \frac{2\hat{\epsilon}}{\sinh(2\hat{\epsilon})}$$

Another form of Eq. (2.11) is obtained by solving it for $\hat{\epsilon}$.

$$\hat{\epsilon} = \frac{\chi^2 S}{3} \left[\frac{1}{1 - \nu^2} (1 + \hat{\beta}^2 / \chi^2)^2 - f(\hat{\epsilon}) \right] \quad (2.13)$$

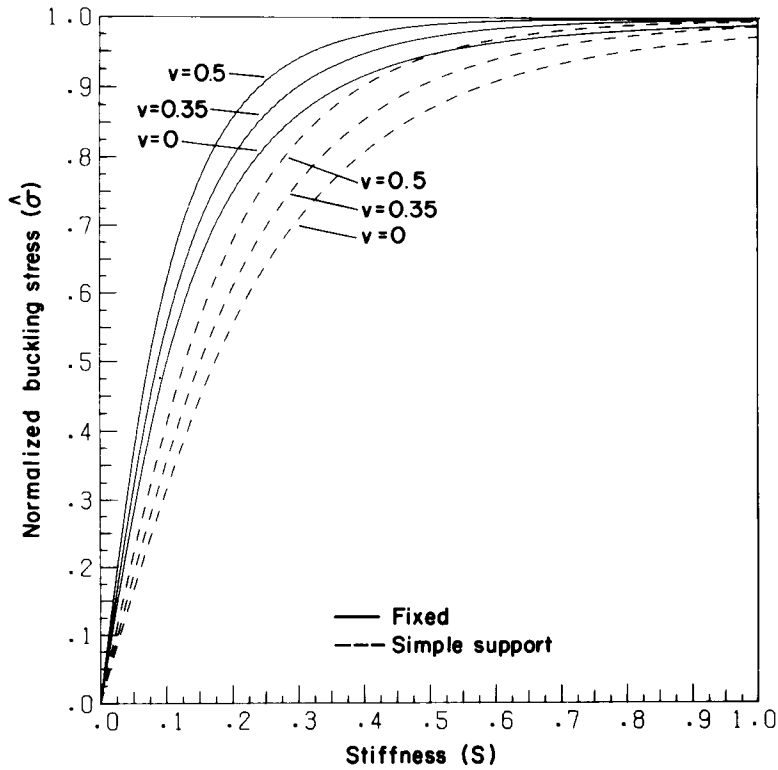


FIG. 2. Plots of $\hat{\sigma}$ as a function of S for three mean Poisson's ratios and two edge-support conditions. (ML85 5255)

SIMPLY SUPPORTED EDGES

The boundary conditions for simple support are

$$x = \pm b : W = \frac{\partial^2 W}{\partial x^2} = 0 \quad (3.1)$$

In solution (2.7), these boundary conditions lead to $a_1 = 0$ and $\hat{\beta} = \pi/2$ for the lowest mode. Setting $\hat{\beta} = \pi/2$ in Eq. (2.13) you obtain the equation

$$\hat{\epsilon} = \frac{\chi^2 S}{3} \left[\frac{1}{1 - \nu^2} \left(1 + \frac{\pi^2}{4\chi^2} \right)^2 - f(\hat{\epsilon}) \right] \quad (3.2)$$

To determine the value of χ that minimizes $\hat{\epsilon}$, differentiate (3.2) with respect to χ and set $d\hat{\epsilon}/d\chi = 0$ to obtain

$$\chi = \frac{\pi}{2} [1 - (1 - \nu^2)f(\hat{\epsilon})]^{-1/4} \quad (3.3)$$

Substituting χ from (3.3) back in (3.2) yields an equation for the critical buckling strain,

$$\hat{\epsilon} = \frac{\pi^2}{6(1 - \nu^2)} S \{1 + [1 - (1 - \nu^2)f(\hat{\epsilon})]^{1/2}\} \quad (3.4)$$

Equation (3.4) is solved by fixed-point iteration where $\hat{\epsilon}$ is initialized according to the solution of the linearized theory,

$$\text{Initial } \hat{\epsilon} = \frac{\pi^2 S}{3(1 - \nu^2)} \quad (3.5)$$

Knowing $\hat{\epsilon}$, the dimensionless wave number χ can be obtained from (3.3). Results of this calculation for normalized buckling strain and stress, assuming simple-support edge conditions, are shown in Figs. 1 and 2.

FIXED EDGES

The boundary conditions for fixed edges are

$$x = \pm b: W = \frac{\partial W}{\partial x} = 0 \quad (4.1)$$

In order for the solution of Eq. (2.7) to satisfy the conditions in Eq. (4.1) for nonzero a_1 and a_2 , we must have

$$\hat{\beta} \tan \hat{\beta} + \hat{\alpha} \tanh \hat{\alpha} = 0 \quad (4.2)$$

The problem is to solve Eqs. (2.12), (2.13), and (4.2) for $\hat{\alpha}(\chi)$, $\hat{\beta}(\chi)$, and $\hat{\epsilon}(\chi)$ and then to minimize $\hat{\epsilon}(\chi)$ with respect to χ . To construct a convergent numerical procedure to accomplish this task we start by rearranging Eq. (4.2) to

$$\hat{\beta} = \tan^{-1}(-\hat{\alpha} \tanh \hat{\alpha} / \hat{\beta}) + \pi \quad (4.3)$$

The \tan^{-1} function returns the principal value in Eq. (4.3). The constant π is added so that the branch of the inverse tangent that corresponds to the lowest buckling load is used. Substituting $\hat{\alpha}$ from Eq. (2.12) into Eq. (4.3) gives

$$\hat{\beta} = \tan^{-1}[-(\hat{\beta}^2 + 2\chi^2)^{1/2} \tanh(\hat{\beta}^2 + 2\chi^2)^{1/2} / \hat{\beta}] + \pi \quad (4.4)$$

In principle, Eqs. (2.13) and (4.4) are to be solved for $\hat{\epsilon}$ and $\hat{\beta}$ as functions of χ^2 and then $\hat{\epsilon}$ minimized with respect to χ^2 . As this procedure is difficult to implement, we modify it by adding an equation expressing the fact that $d\hat{\epsilon}/d\chi^2 = 0$. The result is three equations for $\hat{\epsilon}$, $\hat{\beta}$ and χ , which are to be solved by an appropriate iteration procedure.

Square both sides of Eq. (2.11) and differentiate with respect to χ^2 using $d\hat{\epsilon}/d\chi^2 = 0$. Combining the result with Eq. (2.11) you get

$$\chi = \left[\frac{\hat{\beta}^4 - 2\hat{\beta}\hat{\beta}'\chi^4}{2\hat{\beta}^3\hat{\beta}' - \hat{\beta}^2 + 1.5(1 - \nu^2)\hat{\epsilon}/S} \right]^{1/2} \quad (4.5)$$

where $\hat{\beta}' = d\hat{\beta}/d\chi^2$. An equation for $\hat{\beta}'$ is obtained by differentiating Eq. (4.2).

$$\hat{\beta}' = - \frac{\tanh \hat{\alpha} / \hat{\alpha} + 1 / \cosh^2 \hat{\alpha}}{\tan \hat{\beta} + \hat{\beta} / \cos^2 \hat{\beta} + (\hat{\beta} / \hat{\alpha}) \tanh \hat{\alpha} + \hat{\beta} / \cosh^2 \hat{\alpha}} \quad (4.6)$$

The result is three equations for $\hat{\epsilon}$, $\hat{\beta}$, and χ , (2.13), (4.4), (4.5) (with (2.12) and (4.6) used to calculate $\hat{\beta}'$), which are solved by iteration as follows:

1. Input stiffness parameter S and mean Poisson's ratio ν .

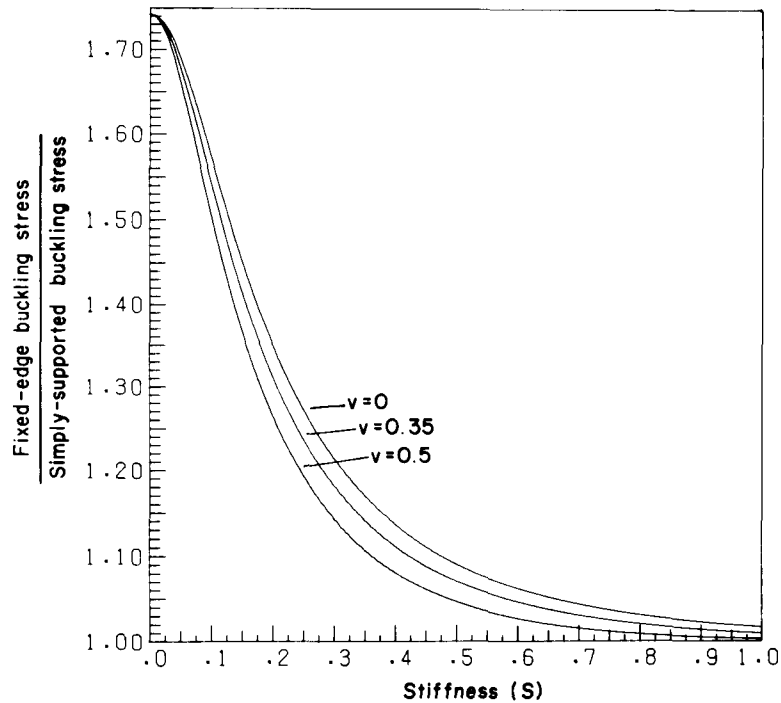


FIG. 3. Ratio of fixed-edge buckling stress to simply-supported buckling stress as a function of S for three mean Poisson's ratios. (ML85 5256)

2. Initialize $\hat{\epsilon}$, χ , and $\hat{\beta}$ as simple support values.
3. Use Eq. (4.4) to improve $\hat{\beta}$ by fixed point iteration.
4. Use Eq. (2.13) to improve $\hat{\epsilon}$ by fixed point iteration.
5. Compute $\hat{\beta}'$ by Eqs. (2.12) and (4.6). Use Eq. (4.5) to improve χ .
6. If χ has converged, output. If χ has not converged, start at 3 again.

Results of this calculation for normalized buckling strain and stress, assuming fixed-support edge conditions, are shown in Figs. 1 and 2.

RESULTS

On Figs. 1 and 2 are shown the normalized buckling strain and stress, respectively, as functions of the dimensionless stiffness S and mean Poisson's ratio ν for the fixed-edge and simply-supported plate conditions. The normalized buckling stress, from Eq. (0.1), is given by

$$\hat{\sigma} = \sigma/c_1 = \tanh \hat{\epsilon} \quad (5.1)$$

The calculations illustrated on Fig. 2 assume that the material is elastic for all values of S . In practice, failure will also occur when $\hat{\sigma}$ reaches its ultimate value $\hat{\sigma}_u = \sigma_u/c_1$, where σ_u is the ultimate compressive stress of the material. Hence, $\hat{\sigma}_u$ provides an upper bound for $\hat{\sigma}$. When $\hat{\sigma} < \hat{\sigma}_u$, failure occurs by elastic buckling according to Fig. 2. For paperboard, the data on σ_u and c_1 reported by Urbanik (1981) indicate $\hat{\sigma}_u \sim 0.9$. Call S_u the value of S corresponding to $\hat{\sigma}_u$. S_u depends

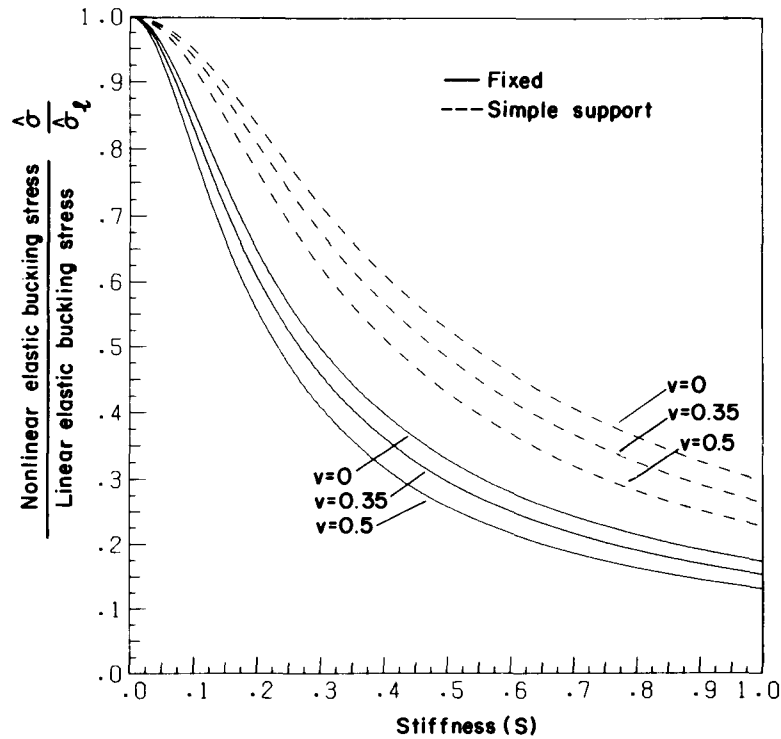


FIG. 4. Ratio of nonlinear elastic buckling stress to linear elastic buckling stress as a function of S for three mean Poisson's ratios and two edge-support conditions. (ML85 5257)

on ν and whether the edges are fixed or simply supported. If $S < S_u$, failure by elastic buckling will occur. If $S > S_u$, failure by compression will occur when $\hat{\sigma} = \hat{\sigma}_u$.

from Fig. 2 we see that for $\hat{\sigma} = \hat{\sigma}_u = 0.9$, $S = S_u$ is in the interval $0.241 < S_u < 0.575$. Stiffness of corrugated fiberboard components is on the order of $0.2 < S < 0.5$. Hence, for these components, the mechanism of failure depends on the nature of the edge restraint, which will lie between fixed and simple support, and the mean Poisson's ratio.

In corrugated fiberboard the plate components have an edge restraint that lies between simple and fixed support. In Fig. 3 is shown the ratio of fixed-edge buckling stress to simple-supported buckling stress as a function of stiffness. Our theory predicts that as stiffness decreases the buckling strength becomes more sensitive to the restraint offered by adjoining components.

The linear stress-strain law $\sigma = c_2 \epsilon$, or $\hat{\sigma} = \hat{\epsilon}$, agrees with Eq. (0.1) for small strains. For a small strain $f(\hat{\epsilon}) = 0(\hat{\epsilon}^2)$ so that Eq. (2.13), the linear buckling stress, is

$$\hat{\sigma}_\ell = CS \quad (5.2)$$

where

$$C = \frac{\chi^2}{3} \left[\frac{1}{1 - \nu^2} (1 + \hat{\beta}^2 / \chi^2)^2 \right] \quad (5.3)$$

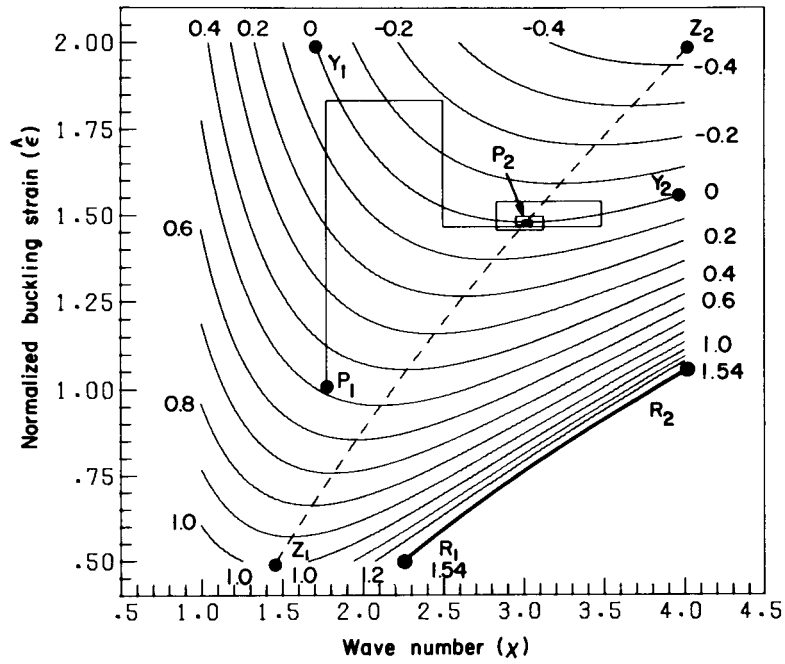


FIG. 5. Contours of function $g(\epsilon, \chi)$ for the fixed edge plate with $S = 0.3$ and $\nu = 0.35$. The fixed point iteration proceeds from point P_1 to point P_2 . The contour Y_1, Y_2 is $g = 0$. The points along the path Z_1, Z_2 satisfy $\partial g / \partial \chi = 0$. (ML85 5258)

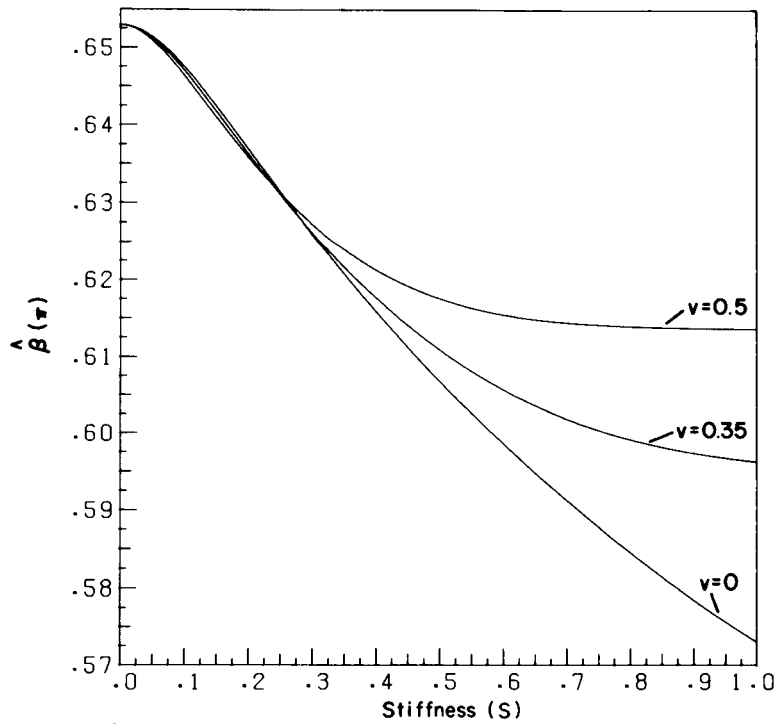


FIG. 6. Plots of $\hat{\beta}$ as a function of S for the fixed-edge case and three mean Poisson's ratios. The ordinate values are multiples of π . (ML85 5259)

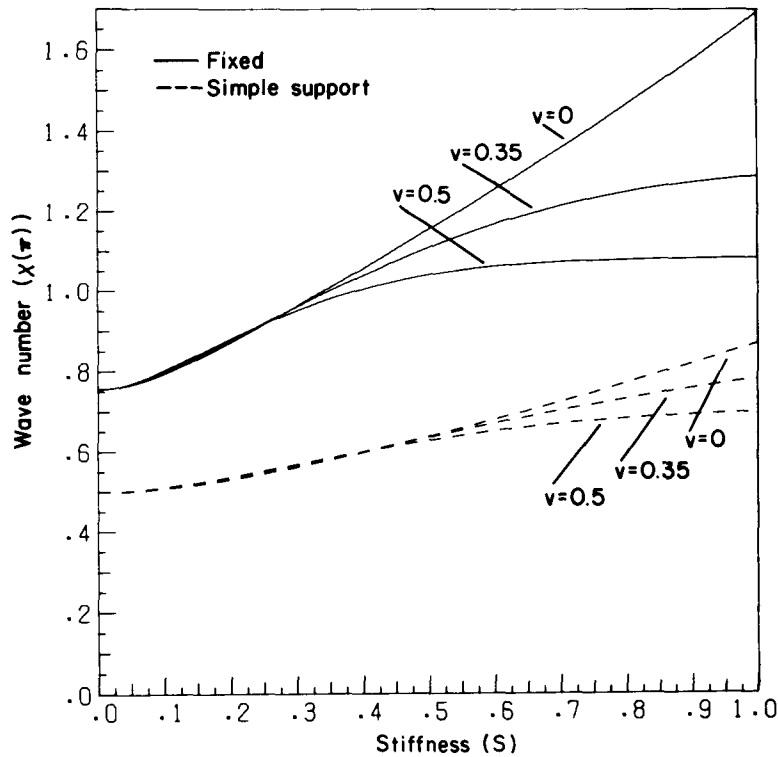


FIG. 7. Plots of χ as a function of S for three mean Poisson's ratios and two edge-support conditions. The ordinate values are multiples of π . (ML85 5260)

For simple support $\hat{\beta} = \pi/2$ and Eq. (3.3) gives $\chi = \pi/2$. Hence, in this case

$$C = \frac{\pi^2}{3(1 - \nu^2)}$$

which makes Eq. (5.2) agree with Eq. (3.5) as it should. For fixed edges, $\hat{\beta}$ and χ are determined by the same iteration used for the nonlinear case, with $\hat{\epsilon}/S$ in Eq. (4.5) replaced by C which is calculated from (5.3).

Figure 4 shows the ratio of nonlinear elastic buckling stress to linear elastic buckling stress given by (5.2). For values of S found in fiberboard components, note the importance of accounting for nonlinearity in the stress-strain relation.

For the fixed edge plate, the steps in the fixed point iteration corresponding to plate properties $S = 0.3$ and $\nu = 0.35$ follow the path shown in Fig. 5. Point P_1 , with coordinates $\chi = 1.78$, $\hat{\epsilon} = 1.00$, is the initial point corresponding to the simply supported plate. The iteration converges to point P_2 with coordinates $\chi = 3.02$, $\hat{\epsilon} = 1.48$.

Also shown on Fig. 5 are contour curves for functions $g(\hat{\epsilon}, \chi)$ equal to $\hat{\beta}$ (given by Eq. (4.4)) minus $\hat{\beta}$ (given by Eq. (2.11)). The contour Y_1Y_2 is $g = 0$ on which the solution P_2 lies at $\hat{\epsilon}$ equal to the minimum. The contours attain a minimum with respect to χ along curve Z_1Z_2 where $\partial g/\partial \chi = 0$. Paths Y_1Y_2 and Z_1Z_2 intersect at the solution P_2 . Below and to the right of R_1R_2 is a region where g is complex. Above and to the left of R_1R_2 g is real.

Root $\hat{\beta}$ for the fixed edge plate is shown in Fig. 6. Recall that $\hat{\beta} = \pi/2$ for the simply supported plate. Normalized wave number χ is shown on Fig. 7.

Finally, we note that the relevant dimensionless material constants are the stiffness S and mean Poisson's ratio ν . Because S , as given by Eq. (2.10), contains the term for plate thickness, h , we can presumably measure h . In this respect, the effective-thickness concept proposed by Setterholm (1974) and examined by Rosenthal (1977), based on combining tensile and bending data measured independently, seems applicable.

CONCLUSIONS

The facings and flutes of corrugated fiberboard are flexible enough to buckle locally under edgewise compression. The flutes retard adhesive-line rotation, stiffening the facings' edges and strengthening the entire board structure. Low stiffness facings gain or lose strength the most from a change in flute stiffness. Variations in flute material will cause a corresponding variance in fiberboard edgewise compressive strength. That strength variation will likely increase as the facings absorb moisture and become less stiff and therefore more sensitive to the flutes. This explains one difficulty with predicting the stacking life of corrugated containers under humid conditions. The converse situation of the facings stabilizing the flutes also arises.

Use of nonlinear load-deformation response of paperboards leads to predictions of lower buckling loads than does use of linear material response, and becomes more significant with stiff components. Material nonlinearity needs to be accounted for in fiberboard strength formulas, especially when the components vary in stiffness. Fiberboard strength may correlate with its components' compressive strengths by virtue of a fortuitous correlation between paperboard strength and stiffness. But if developed around a narrow range of stiffnesses, those formulas that ignore material nonlinearity are likely to fail upon extrapolation to encompass many paperboard grades varying in stiffness.

Our analysis of a thin plate considers two cases of edge restraint. Numerical procedures are given for solving the buckling equations that arise from solving the equilibrium conditions and boundary conditions. A graph of the iteration shows how convergence occurs in the case of fixed edges.

REFERENCES

- JOHNSON, M. W., JR., AND T. J. URBANIK. 1984. A nonlinear theory for elastic plates with application to characterizing paper properties. *J. Appl. Mech.* 51:146-152.
- , ———, AND W. E. DENNISTON. 1979. Optimum fiber distribution in singlewall corrugated fiberboard. USDA Forest Serv. Res. Pap. FPL 348, Forest Prod. Lab., Madison, WI.
- ROSENTHAL, M. R. 1977. Effective thickness of paper: Appraisal and further development. USDA Forest Serv. Res. Pap. FPL 287, Forest Prod. Lab., Madison, WI.
- SETTERHOLM, V. C. 1974. A new concept in paper thickness measurement. *Tappi* 57(3):164.
- URBANIK, T. J. 1981. Effect of paperboard stress-strain characteristics on strength of singlewall corrugated fiberboard: A theoretical approach. USDA Forest Serv. Res. Pap. FPL 401, Forest Prod. Lab., Madison, WI.